J. Sens. Sens. Syst., 2, 19–26, 2013
www.j-sens-sens-syst.net/2/19/2013/
doi:10.5194/jsss-2-19-2013

JSSS Journal of Sensors and Sensor Systems Open Access

Driving modes and material stability of a double membrane rheometer and density sensor

B. Weiss, M. Heinisch, E. K. Reichel, and B. Jakoby

Institute of Microelectronics and Microsensors, Johannes-Kepler University, Linz, Austria

Correspondence to: B. Weiss (weiss_bernhard@gmx.at)

Received: 13 December 2012 – Revised: 18 March 2013 – Accepted: 23 March 2013 – Published: 22 April 2013

Abstract. This contribution presents the analysis of an earlier proposed double membrane sensor for measuring mass density and rheological properties of liquids with respect to different driving modes. Concerning practical implementation the sensor mounting and the stability of the polyethylene foil, currently used as membrane material, are investigated. The sensor is based on two opposed membranes vibrating in parallel where a sample liquid is enclosed between the membranes. The excitation and read-out mechanisms of the membrane vibration are based on Lorentz forces induced in a static magnetic field. Each membrane carries three conductive paths for excitation, which can be separately connected to the excitation currents. This allows the excitation of the first and second modes of vibration and enables prestressing the second mode of oscillation. Analyzing the material-stability of the used polyethylene foil shows a strong long-term drift of the modulus of elasticity and an increase of internal damping with increasing temperature. Comparing the resonance frequency of the fundamental mode with earlier measurements achieved with the second mode of resonance indicates an increased sensitivity to density featuring a reasonably sustained quality factor for high viscosities. Thereby, the sensitivity can be adjusted by varying the distance between the membranes.

1 Introduction

In recent years an increasing need for in-line sensing of fluid parameters like mass density and viscosity in industrial and biomedical fields can be observed (Jakoby et al., 2009). Whereas conventional rheometers offer good measurement results and applicability in the laboratory environment, miniaturized sensors are needed for the in-line fluid parameter monitoring. Among those, the vibrational behavior of e.g., tuning forks shows a high dependence on fluid properties with high coupling and cross-sensitivities among mass density and viscosity (Blaauweegers et al., 2007). On the other hand, capillary tube on-chip viscometers have been found to be an effective means for determining the shear viscosity of highly viscous liquids by means of evaluating the pressure drop necessary for inducing a laminar channel flow (Lin et al., 2007; Chevalier and Ayela, 2008; Wang et al., 2010). Furthermore, viscosity variations may be determined by evaluating the propagation of acoustic waves through a microchannel filled with the test liquid (Choi et al., 2010). Quartz-crystal thickness shear mode resonators, which work in the high kHz range, are already very popular for the fluid parameter sensing of thin interfacial films (Kanazawa and Gordon, 1985; Kanazawa, 1997). In the industrial and biomedical environment complex multicomponent fluids like oil emulsions or blood, which are characterized by length-scales of several micrometers, need to be measured. In order to increase the amount of the moved sample liquid and the penetration depth of excited shear waves, ultimately macroscopic devices have been designed that operate in the low kHz range (Blaauweegers et al., 2007; Jakoby et al., 2009). Recently, such a miniaturized rheometer was proposed, which is based on two opposed polyethylene (PE) membranes that vibrate in parallel in the test liquid (Reichel et al., 2007). The vibration is induced by the Lorentz forces on two excentric conductive paths in a static magnetic field. The vibration characteristics of the membranes, in particular resonance frequency and quality factor of the eigenmodes, directly depend on the rheological properties of the enclosed fluid volume; namely, its mass density ρ_f

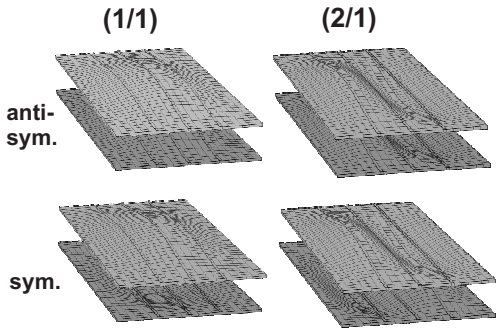

Figure 1. The symmetrical and antisymmetrical vibration of the two opposed membranes in the fundamental (1/1) mode and in the second (2/1) mode.

and dynamic viscosity μ. The second mode of vibration, see Fig. 1, was analyzed in Heinisch et al. (2011) where different sensitivities on density and viscosity for symmetric and antisymmetric excitation have been observed.

In the case of the symmetric mode of excitation, the induction of shear waves in the sample liquid couples the fluid viscosity to the change of the membrane vibration characteristics. An analytical study of shear waves shows that the damping force on the membrane depends on the square root of the dynamic viscosity times mass density $\sqrt{\rho_f \mu}$ (Kanazawa, 1997). Consequently, in order to determine the dynamic viscosity, the mass density needs to be obtained from a different measurement. This poses the question if there are driving modes of the double membrane configuration that are not characterized by this strong density–viscosity coupling.

In this contribution the previous membrane design is extended by a third centered conductive excitation path. This offers, first, the excitation of the first mode of resonance. It will be shown that this mode is characterized by a high sensitivity to density at low viscous damping, where the sensitivity on viscosity depends on the sensor geometry and driving frequency. Second, a constant current through the center driving conductive path can be used to deflect and prestress the membrane, which changes the frequency of the second mode.

Miniaturizing viscosity and density sensors aims at the large-scale production and the application in industrial environments. Therefore, also the topics of material stability, temperature dependency and long-term drift of the used material are addressed.

In Sect. 2 the sensor principle and the test arrangement are shown, the vibrational behavior is discussed in Sect. 3 and modeled in Sect. 4, the stability of the used PE foil is discussed in Sect. 5, measurements of different driving modes are shown in Sect. 6, and Sect. 7 finally concludes the work.

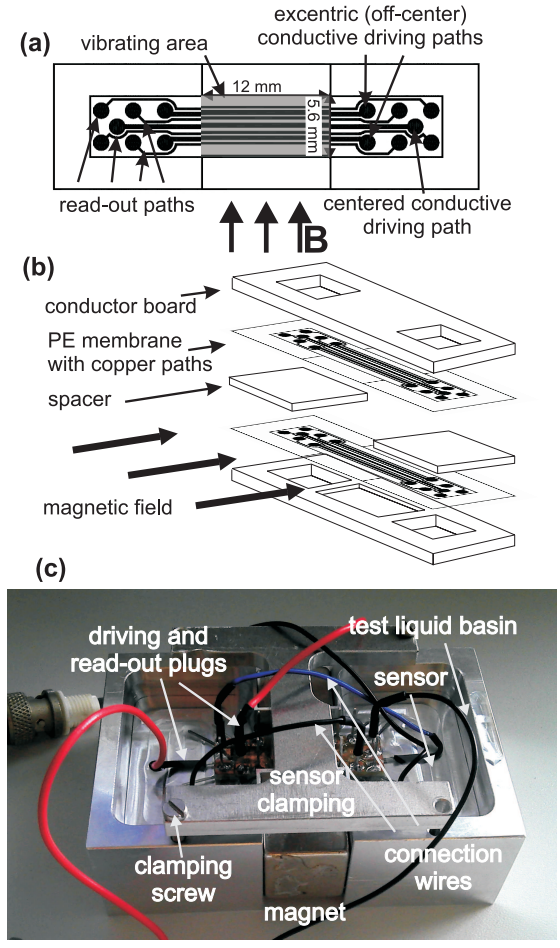

Figure 2. In **(a)**, the design of the PE membrane and the arrangement of the excitation and read-out paths are shown. **(b)** shows the assembly of the double membrane sensor and **(c)** depicts the measurement setup.

2 Sensor principle and fabrication

2.1 Composition and fabrication

In Fig. 2a the vibrating membrane is shown. By means of photolithographic processes electric conductive paths are realized in copper on a 100 µm thick polyethylene (PE) foil. Each membrane carries a centered main conductive path for the excitation of the first (1/1) mode of vibration, see Fig. 1. The two excentric (off-center) conductive excitation paths are used to excite the second (2/1) mode of vibration. Furthermore, the design features conductive read-out paths. The voltage induced in the path when vibrating in the static magnetic field is used to evaluate the deflection of the membrane.

Figure 2b depicts the sensor setup. The membranes are glued to conductor boards using epoxy. Two membranes are assembled and by means of further layers of PE foil between the two membranes the distance between them is varied. In order to achieve different driving modes, the electric paths

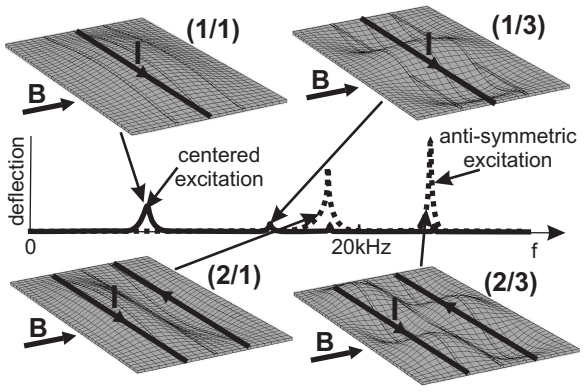

Figure 3. Shows modes of a single clamped membrane vibrating in vacuum – the numeric simulation is done with Comsol 4.1. The dashed line describes the response of the membrane to the excitation by the two excentric paths, where the (2/1) and the (2/3) modes are driven. Applying a harmonic current to the center-path excites the (1/1) and the (1/3) modes.

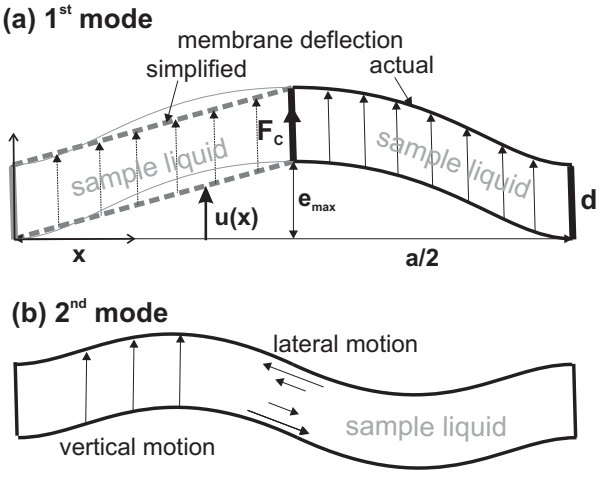

Figure 4. Qualitative two-dimensional flow between the two membranes, when vibrating antisymmetrically in the first **(a)** and in the second mode of vibration **(b)**.

may be individually joined by external connection wires, see Fig. 2c.

2.2 Principle

In the presence of an external static magnetic field perpendicular to the electric paths, currents through the excitation path result in Lorentz forces that deflect the membrane. By means of harmonic currents through the paths, a vibration of the membrane is excited. The read-out mechanism is based on the measurement of voltage u_{ind} that is induced in the thinner read-out paths:

$$u_{\mathrm{ind}} = \int_l \boldsymbol{v} \times \boldsymbol{B} \cdot \mathrm{d}\boldsymbol{s}, \tag{1}$$

where l, $\boldsymbol{v}$ and $\boldsymbol{B}$ are the total length of the read-out paths, the velocity vector of the vibrating electric path and the magnetic flux density, respectively.

2.3 Sensor arrangement and measurement setup

The sensor is placed in a basin containing the test liquid between two permanent magnets, which provide field strengths of up to 0.2 T, see Fig. 2c. Liquid laterally enters the gap between both membranes. The connection of the excitation paths, which determines the excited vibration mode, is configured by the connection wires. The excitation paths are connected to a function generator, where GPIB (General Purpose Interface Bus) controlled frequency sweeps with an amplitude of approximately 0.5 V are used to evaluate the frequency response of the membrane vibration. The induced read-out voltage is measured with a Stanford Research lock-in amplifier SR 830.

3 Vibrational behavior

The vibration of the double membrane configuration can be regarded as the vibration of two single membranes that are coupled by external loads depending on the properties and the resulting flow of the adjacent liquid. The load consists of an added mass, which corresponds to the fluid mass that is periodically accelerated by the membrane vibration. The viscous loss caused by the periodic shear deformation of liquid layers adjacent to the membrane surface effects a damping of the membrane motion.

3.1 Vibration modes

By applying a time-harmonic electric current to the centered path, the longitudinal (1/1) and (1/3) modes are excited, see Fig. 3. The (n/m) mode therein describes the membrane vibration with the n-th mode in lateral and the m-th mode in longitudinal direction. The lateral (2/1) and (2/3) high frequency modes are excited by using the excentric paths. In practice, a slight asymmetry of the membrane shape or the driving currents causes that all modes may occur in spite of a selective excitation.

While the applicability of the higher order (2/1) vibration mode for the coupled viscosity–density sensing has already been proven (Heinisch et al., 2011), this paper proposes the use of the first (1/1) vibration mode for efficient mass-density sensing.

3.2 Liquid loading

Figure 4 qualitatively shows the flow between the two membranes. In the case of the first mode, see Fig. 4a, the liquid predominantly is moved vertically. In contrast, when vibrating in the second mode as presented in Heinisch et al. (2011),

see Fig. 4b, the flow is characterized by the superposition of the vertical motion and the lateral shear motion in the area between the two peaks. The lateral flow components transport liquid from the crest to the valley of the deflection. The amount of lateral shear components increases with the distance between the two membranes.

The vertical fluid motion in the case of the fundamental mode vibration exerts two effects on the membrane. First, the fluid layer that is periodically moved between the two membranes acts as added mass that in addition to the mass of the membrane needs to be periodically accelerated by the driving force. Second, there is a shear force between adjacent vertical fluid layers. This force scales with the fluid viscosity and dampens the membrane vibration.

The comparision of the energies associated with the inertial and the viscous motion of the liquid is given in terms of the quality factor Q_f, which describes the damping of the resonant vibration due to the viscous liquid:

$$Q_\mathrm{f} = \frac{\omega \hat{W}'_\mathrm{kin}}{\overline{P}'_D}. \tag{2}$$

Therein, ω is the angular velocity of the vibration, $\hat{W}'_\mathrm{kin}$ describes the peak kinetic energy of the liquid layer and $\overline{P}'_D$ denotes the average power related to the dissipative viscous flow components over one period of oscillation, i.e., the power required to drive the two Couette flows, see Fig. 4a. The two components may easily be evaluated, if the deflection shape of the membrane is approximated by a linear shape as shown in Fig. 4a. The primes ($'$) indicate that these quantities are given per unit length in z-direction in our 2-D model. In this case the vertical shear motion of neighboring fluid slices is described by a simple harmonic Couette flow. Therein,

$$F'_c(t) = d\mu \frac{2}{a} \omega e_\mathrm{max} \sin(\omega t) \tag{3}$$

is the force per unit length needed to induce the Couette flow of one, e.g., the left half of the liquid layer featuring a width $a/2$, where e_max, d and a are the maximum membrane deflection, the gap width between the membranes and the width of the membrane, respectively. The associated velocity in the membrane center is given by $\omega e_\mathrm{max} \sin(\omega t)$, which, at resonance, is in phase with the driving force. The corresponding dissipative power per unit length yields

$$\overline{P}_D = 2\frac{\omega}{2\pi} \int_0^{\frac{2\pi}{\omega}} F'_c(t)\, \omega e_\mathrm{max} \sin(\omega t)\, \mathrm{d}t = 2\mu \frac{d}{a} \omega^2 e_\mathrm{max}^2. \tag{4}$$

Furthermore, we note that the peak velocity (at zero crossing) at position x is given by $v(x) = e_\mathrm{max}\omega \frac{x}{a/2}$. Then, under the same assumption of a simplified deflection shape, the kinetic energy per unit length that is associated with the inertial flow components is obtained as

$$\hat{W}'_\mathrm{kin} = 2 \int_0^{\frac{a}{2}} \frac{1}{2} \rho_\mathrm{f}\, \mathrm{d}\, v(x)^2\, \mathrm{d}x = \frac{a}{6} \mathrm{d} \rho e_\mathrm{max}^2 \omega^2. \tag{5}$$

Evaluating the quality factor from Eq. (2) gives

$$Q_\mathrm{f} = \frac{\omega \hat{W}'_\mathrm{kin}}{\overline{P}_D} = \frac{1}{2} \frac{\rho_\mathrm{f}}{\mu} \omega a^2. \tag{6}$$

Consequently, the Q_f-factor decreases with the kinematic viscosity μ/ρ_f, increases with the driving frequency and increases quadratically with the width a of the membrane. As the fundamental mode of vibration has the greatest lateral extension a this mode offers the highest Q_f, i.e., high sensitivity to mass density at low viscous damping.

In addition to the damping of the vibration due to the viscous liquid, the membrane is subjected to intrinsic damping in the used PE-membrane and damping due the glued mounting of the membrane on the conductor board. The mechanical damping Q_mech is added to the fluid damping Q_f in the following way:

$$\frac{1}{Q_\mathrm{tot}} = \frac{1}{Q_\mathrm{f}} + \frac{1}{Q_\mathrm{mech}}, \tag{7}$$

yielding Q_tot, which quantifies the total damping of the membrane vibration due to mechanical dissipation in the membrane and due to the liquid loading. Evaluating Q_f for the used test liquids given in Table 1 shows that Q_f lies in the order of 10^4–10^5. As the quality factor of the membrane vibration is in the range of 10^1, see the measurements represented in Fig. 8 below, the damping of the membrane vibration due to the fluid's viscosity may be neglected in the case of a perfectly parallel first mode (1/1) vibration of the two membranes.

Table 1. Parameters of test fluids.

Liquid	ρ_f [kg m^{-3}]	μ [mPa s]	$f_{\mathrm{f},11}$ [s^{-1}]
Air	1.2	0.017	9696
2-Prop.	780	2.41	8343
Acetone	790	0.33	8238
DI water	1000	1.0	7943

4 Modeling

4.1 Membrane vibration

Recently, the membrane vibration and the fluid flow between the two membranes was analyzed by means of a seminumerical three-dimensional computation based on a Green function approach applied to the linearized Navier–Stokes equations in the spectral domain (Reichel et al., 2009; Voglhuber-Brunnmaier et al., 2010). In this contribution a simplified analytical model is used, which is based on the analytical value

for the resonance frequency of a thin membrane freely vibrating at the n-th transversal mode and the m-th longitudinal mode, fixed at the four borders $\omega_{0,nm}$ (Reddy, 2007):

$$\omega_{0,nm} = \sqrt{\frac{D\pi^4}{2\rho_m h}\left(\frac{n}{a}+\frac{m}{b}\right)^2} \text{ with} \quad (8)$$

$$D = \frac{EH^3}{12(1-\nu^2)}. \quad (9)$$

This interrelation predicts that the resonance frequency of the double membrane configuration decreases with increasing fluid density and gap width.

Here, ρ_m, E, ν and b are the density of the membrane foil, Young's modulus, Poisson's ratio and the length of the membrane, respectively.

4.2 Liquid loading

Considering that the quality-factor due to the liquid loading Q_f is in order of 10^4 for the liquids to be measured, the effect of the viscous damping on the resonance frequency can be neglected. The added mass of moved fluid layer can simply be regarded as an increased foil mass density, thereby each membrane has to carry half of the liquid mass:

$$\omega_{f,nm}=\omega_{0,nm}\left[1+\frac{d}{2h}\frac{\rho_f}{\rho_m}\right]^{-\frac{1}{2}} = \sqrt{\frac{D\pi^4}{2(\rho_m h+\rho_f d/2)}}\left(\frac{n}{a}+\frac{m}{b}\right)^2. \quad (10)$$

5 Material stability

The proposed sensor concept in principle can be implemented using different materials for the membrane. PE foils feature several advantages. First, due to their elasticity, the required driving current can be reduced. Second, they can be processed in a simple manner and would yield low cost in production. At the same time, polymer materials show adverse properties in terms of aging or mechanical stability in general compared to standard micromachining materials. In this section we report on corresponding investigations that have to be included when the feasibility of this technology is evaluated for a particular application.

To investigate the properties of the material as a mechanically vibrating component in a device, we decided to use a simpler vibrating structure in order to eliminate additional issues that are associated with the clamping of the membrane boundary and thus obtain a better insight on the material properties themselves. Thus, we studied the mechanical stability of the used polymer material by investigating the resonance properties of a simple cantilever operating in the fundamental mode of vibration. It is made of the same PE material and has similar geometrical dimensions as the membrane. Using a cantilever rather than a membrane reduces the influences associated with the clamping, which are expected to be another significant factor in case of a membrane.

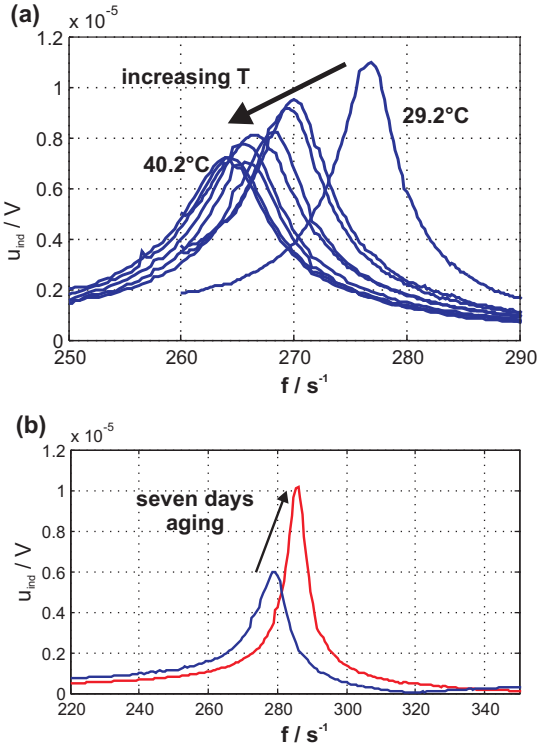

Figure 5. Analysis of the first vibration mode of a $12\times4\,\text{mm}^2$ PE cantilever. **(a)** shows the decrease of resonance frequency and quality factor due to membrane heating. In **(b)**, the increase of the resonance frequency due to membrane aging is demonstrated.

The used PE foil is subject to various effects that influence the material parameters and consequently the vibration behavior of the sensor. Figure 5a shows that heating the membrane essentially lowers the resonance frequency. There may be various effects causing this decrease: (i), there is a heat induced decrease of the Young modulus of elasticity, and (ii) heating leads to a volumetric expansion of the cantilever, which also lowers the resonance frequency. When cooling down the device, these effects again decrease but there persists a small change of the resonance behavior indicating a persistent change of the polymer structure.

Figure 5b shows that aging has a substantial effect on the membrane vibration characteristics. Within one week of aging in ambient conditions the resonance frequency increases by 4 %. It is supposed that aging caused a volatilization of the softening agents present in the foil. This may influence the resonance frequency in two ways. First, this diffusion decreases the area density of the foil. Second, the absence of the softeners leads to an increased modulus of elasticity.

Considering the heating of the membrane, Joule heating may be of great relevance. Typical parameters of a path resistance of $R = 5\Omega$ and a driving voltage of $V = 0.5$ V rms results in a heating power of $P_H = V^2/R = 0.05$ W. If we assume a sample volume of 1 mL and a typical measuring time of 1 min, the temperature of the test liquid globally rises by

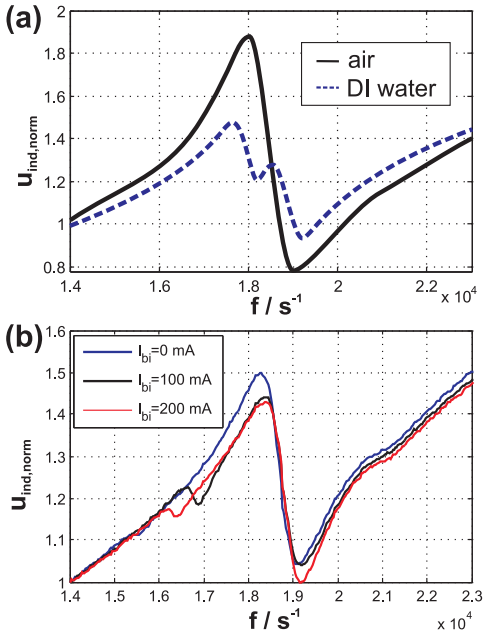

Figure 6. Normalized induced voltage over the excitation frequency, comparing the vibration in air and in DI water, see **(a)**. In **(b)**, the frequency response for the vibration in air is analyzed for the case that a prestress is applied to the foil by means of a bias current on the centered electrode path.

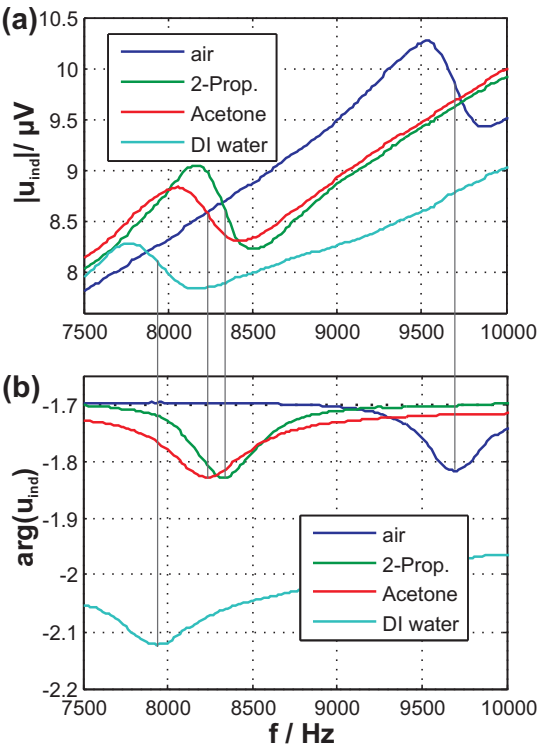

Figure 7. Amplitude **(a)** and phase **(b)** of the frequency response of the double-membrane sensor for various test liquids.

0.7 K, if water with a heat capacity of $c_p = 4.19\,\mathrm{kJ\,kg^{-1}\,K}$ is taken as test liquid.

This is only a very crude estimate of course. On the one hand, the liquid is not thermally insulated from the environment (as implicitly assumed here), on the other hand, there will be temperature differences between the membrane and the bulk of the liquid. So if larger measurement times are required, the local heating of the fluid enclosed by the membranes needs to be considered, i.e., the temperature of the actually measured fluid sample can be significantly different from the ambient temperature. In those cases pumping of the liquid can reduce the effects of local heating without affecting the sensing process.

6 Measurements

6.1 Second mode of vibration with constant prestress

First, the standard vibration of the (2/1) mode is analyzed. In order to eliminate the influence of mutual influences between two membranes, which due to fabrication tolerances are not completely equal, this measurement has been carried out in a single membrane configuration (Weiss et al., 2011) in ambient air. Figure 6a shows the resulting vibration characteristics. Concerning the applicability of this vibration mode for fluid sensing it has to be regarded that upon immersion in water the membrane features lower resonance frequencies, a lower resonance peak and a lower quality factor compared to the vibration in air. A detailed analysis of the respective interaction between test liquid and membrane has been carried out (Reichel et al., 2009).

When applying a constant current to the centered path in addition to the harmonic current through the excentric paths, the membrane is prestressed while vibrating in the second mode. Measurements show two effects for this driving mode, see Fig. 6b. Firstly, with increasing bias current the amplitude of the (2/1) mode decreases whereas the peak of the (1/3) mode increases. Secondly, prestressing the membrane shifts the (2/1) mode to slightly higher frequencies.

It is shown that prestressing influences the vibration characteristics but the desired frequency shift is too small to use this effect for sensor calibration or to change the sensitivity.

6.2 First mode of vibration

Figure 7 shows the evaluation of the resonance behavior of the predominantly density-sensitive first mode of vibration (1/1). The nominal fluid parameters, measured by means of laboratory equipment, and the measured resulting resonance frequencies of the first mode of vibration are given in Table 1. It turns out that the frequency of the first mode essentially decreases with increasing fluid density as predicted by Eq. (10). Furthermore, the quality factor scarcely depends on the fluid viscosity. Phase variations stem from parasitic capacities and conduction phenomena at the electric connections. Exciting

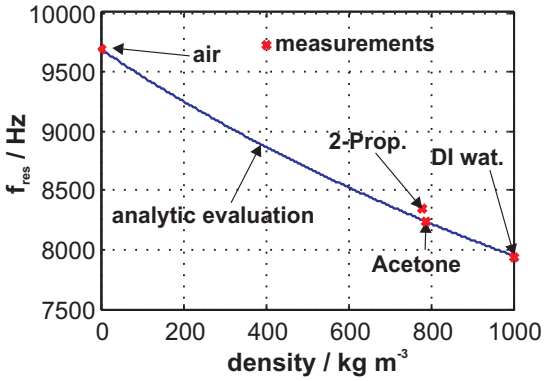

Figure 8. Measured resonance frequencies of different fluids and the respective predictions using Eq. (10), where the Young modulus of the membrane has been fitted to meet the resonance frequency in air.

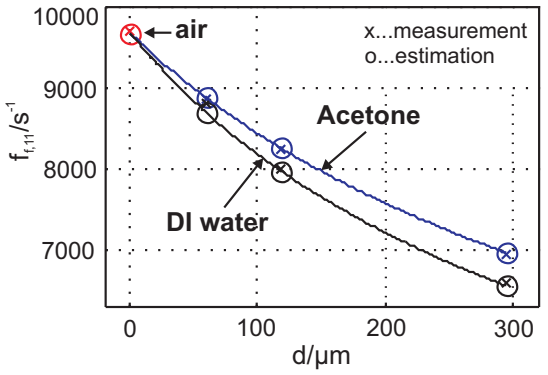

Figure 9. Shows the resonance frequency of the (1/1) mode versus the gap-width d between the membranes for the vibration in air, acetone and water. Measurements are indicated with an (x) and estimations using Eq. (10) are marked by the lines and the (o).

the fundamental mode instead of the second mode yields a higher sensitivity to mass density and a recognizable resonance peak – also for liquids like 2-propanol featuring a somewhat higher viscosity of 2.41 mPa s. The height of the resonance peak scarcely depends on the fluid's viscosity.

Figure 8 shows how the above measurements agree with the estimation made in Eq. (10). We can see that the values for the vibration in acetone and DI (deionized) water are well reproduced by the prediction, which only accounts for the fluid density. The measured resonance frequency for 2-propanol, the fluid with the highest viscosity, is higher than the predicted value. Due to the filling procedure of the test cell and the good wetting properties of the used test liquids, the formation of air bubbles, which would have decreased the added mass, can be excluded. It is thus assumed that the resonance frequency is increased by the component of viscous shear motion of vertical fluid layers, see Fig. 4.

In accordance with the discussion in Sect. 5, other influences like the membrane heating and aging have been observed to essentially influence the vibration behavior. First, an increase of the resonance frequency has been observed in agreement with the measurements carried out with the cantilever. Second, it has been observed that heating essentially decreases the magnitude of vibration. Supposedly, the heating led to a volumetric expansion of the foil, the resulting buckling probably inhibited the free membrane vibration.

6.3 Varying the sensitivity range

When operating in air, the membranes vibrate almost uncoupled, thus, the distance between them virtually does not influence the vibrational behavior. Immersed in a liquid, the vibration of the two membranes is coupled and the gap width determines the amount of liquid load that is moved. Consequently, the resonance frequency essentially depends on the gap width between the membranes, see Eq. (10). In Fig. 9 the influence of the gap width on the frequency shift in comparison to the uncoupled vibration in air is given for DI water, and acetone. The three gap widths have been slightly adapted to fit the measurements. As a result, the measured frequency shift between acetone and DI water is properly reproduced by the above estimation for both fluids, see Fig. 9. An increasing gap width increases the frequency shift. Consequently, by varying this distance, the sensitivity of the sensor on density variations of the test liquids, i.e., $\Delta f_r/\Delta\rho_f$, can be adjusted.

7 Conclusions

The double membrane sensors presented earlier (Reichel et al., 2007) were investigated with respect to additional driving modes. Furthermore, the material stability of the used PE foil was studied. It turned out that aging of the foil essentially increases the modulus of elasticity resulting in higher resonance frequencies. In contrast, heating of the membrane increases the internal friction and results in a volumetric expansion of the foil yielding lower resonance frequencies and reduced quality factors. It can be concluded that other materials like glass or new silver membranes need to be used in order to achieve a long-term stable application in large-scale use.

Nevertheless, the PE foil serves well for a basic study of the sensor principle. First, the second mode of vibration was evaluated for the case that a static deflection was induced by means of a constant current through an additional centered driving path. The resulting prestress therein slightly increases the frequency of the second (2/1) mode and additionally excites the (2/3) mode. Second, it was shown that the use of the fundamental mode of vibration is characterized by a simple relation between the mass density of the intermediate fluid layer and the resulting frequency shift, which holds for viscosities below 1 mPa s. In the case of higher fluid viscosities, the resonance frequency is slightly increased due to the internal friction of neighboring fluid layers. Being characterized

by the small influence of the fluid viscosity, the frequency of the first vibrational mode decreases with $[1+\rho_f d/\rho_m 2h]^{-1/2}$. This relation and respective measurements reveal that the sensitivity to fluid density $\Delta f_{f,11}/\Delta\rho_f$ can be adapted by adjusting the gap width.

Hence, by using the fundamental mode of vibration, the double membrane sensor is capable of density sensing featuring an adjustable sensitivity. The next aim is a decoupled determination of fluid density and viscosity by means of evaluating the fundamental driving mode and a higher order mode, which is characterized by a higher sensitivity on viscosity.

Acknowledgements. The authors would like to thank Bernhard Mayrhofer for the membrane fabrication and Johann Katzenmayer for manufacturing mechanical components of the setup. This work was supported by the Austrian Center of Competence in Mechatronics (ACCM).

Edited by: M. J. da Silva
Reviewed by: two anonymous referees

References

Blaauwgeers, R., Blazkova, M., Clovecko, M., Eltsov, V. B., de Graaf, R., Hosio, J., Krusius, M., Schmoranzer, D., Schoepe, W., Skrbek, L., Skyba, P., Solntsev, R. E., and Zmeev, D. E.: Quartz tuning fork: thermometer, pressure- and viscometer for helium liquids, J. Low Temp. Phys., 146, 537–562, 2007.

Chevalier, J. and Ayela, F.: Microfluidic on chip viscometers, Rev. Sci. Instr., 79, 076102, doi:10.1063/1.2940219, 2008.

Choi, S., Moon, W., and Lim, G.: A micro-machined viscosity-variation monitoring device using propagation of acoustic waves in microchannels, J. Micromech. Microeng., 20, 085034, doi:10.1088/0960-1317/20/8/085034, 2010.

Heinisch, M., Reichel, E. K., Dufour, I., and Jakoby, B.: A resonating rheometer using two polymer membranes for measuring liquid viscosity and mass density, Sens. Act. A: Phys., 172, 82–87, 2011.

Jakoby, B., Beigelbeck, R., Keplinger, F., Lucklum, F., Niedermayer, A., Reichel, E. K., Riesch, Ch., Voglhuber-Brunnmaier, T., and Weiss, B.: Miniaturized sensors for the viscosity and density of liquids – performance and issues, IEEE Trans. on Ultrason., Ferroelec., and Freq. Contr., 57, 111–120, 2010.

Kanazawa, K. K.: Mechanical behaviour of films on the quartz microbalance, Faraday Discuss., 107, 77–90, 1997.

Kanazawa, K. K. and Gordon, J. G.: Frequency of a quartz microbalance in contact with liquid, Analyt. Chem., 57, 1770–1771, 1985.

Lin, Y. Y., Lin, C. W., Yang, L. J., and Wang, A. B.: Microviscometer based on electrowetting on dielectric, Electrochim. Acta, 52, 2876–2883, 2007.

Reddy, J. N.: Theory and analysis of elastic plates and shells, CRC Press, Taylor and Francis, 2nd Edn., 2006.

Reichel, E. K., Riesch, Ch., and Jakoby, B.: A novel combined rheometer and density meter suitable for integration in microfluidic systems, Proc. IEEE Sensors, 908–911, ISBN: 1-4244-1262-5, 2007.

Reichel, E. K., Riesch, Ch., Keplinger, F., and Jakoby, B.: Modeling of the fluid–structure interaction in a fluidic sensor cell, Sens. Act. A: Phys., 156, 222–228, 2009.

Voglhuber-Brunnmaier, T., Reichel, E. K., and Jakoby, B.: Characterization of a novel membrane-rheometer utilizing a semi-numerical modelling approach in the spectral domain, Sens. Act. A: Phys., 162, 310–315, 2010.

Wang, J. N. and Tang, J. L.: An optical fiber viscometer based on long-period fiber grating technology and capillary tube mechanism, Sensors, 10, 11174–11188, 2010.

Weiss, B., Heinisch, M., Reichel, E. K., and Jakoby, B.: Driving modes and material stability of a vibrating polyethylene membrane viscosity sensor, Proc. Engin., 25, 176–179, 2011.